Electronic Supplementary Information

Improving colloidal stability and response performances using looped thermal-responsive brushes

Chi Li[a, b], *Jin Jing*[c], *Yanxiong Pan*[*a, b], *Xiangling Ji*[a, b], *Wei Jiang*[*a, b, c]

[a] *State Key Laboratory of Polymer Physics and Chemistry, Changchun Institute of Applied Chemistry, Chinese Academy of Sciences, Changchun 130022, P. R. China*
[b] *School of Applied Chemistry and Engineering, University of Science and Technology of China, Hefei, Anhui 230026, P. R. China*
[c] *School of Materials Science and Engineering, Wuhan Textile University, Wuhan 430200, P. R. China*

**Corresponding authors: weijiang@wtu.edu.cn (Wei Jiang); yxpan@ciac.ac.cn (Yanxiong Pan)*

Table of Contents

Standard Curves of PNIPAAm by HPLC

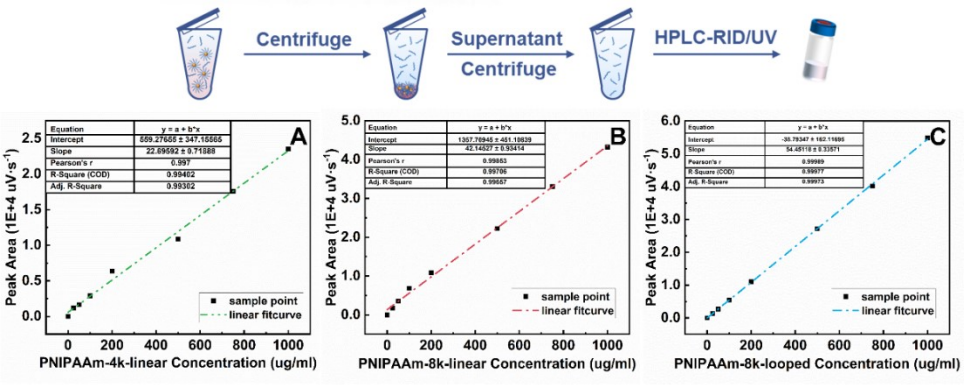

Fig. S1 The standard curve of pure PNIPAAm-4k-linear, PNIPAAm-8k-linear and PNIPAAm-8k-looped in concentration range of 0-1.0 mg ml^{-1}, respectively. And scheme of HPLC quantification analysis of detached PNIPAAm ligands.

Micrographs of Nanoparticles

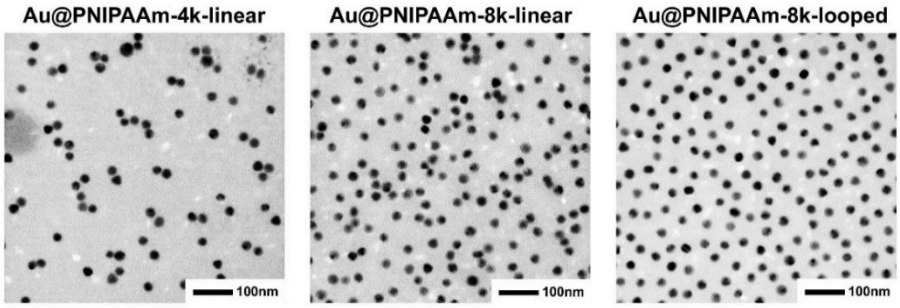

Fig. S2 TEM images of PNIPAAm brush modified samples in scale of 100 nm.

The lighter and unstained indicated polymer shell of the particles, and the high-contrast indicated gold core.

^{1}H-NMR of Nanoparticles

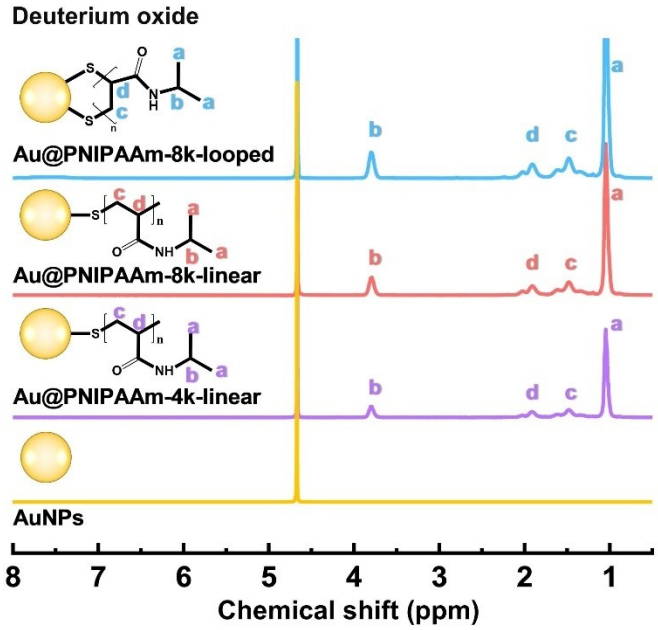

Fig. S3 ^{1}H-NMR spectra of AuNPs, Au@PNIPAAm-4k-linear, Au@PNIPAAm-8k-linear, and Au@PNIPAAm-8k-looped.

FTIR of Polymer and Nanoparticles

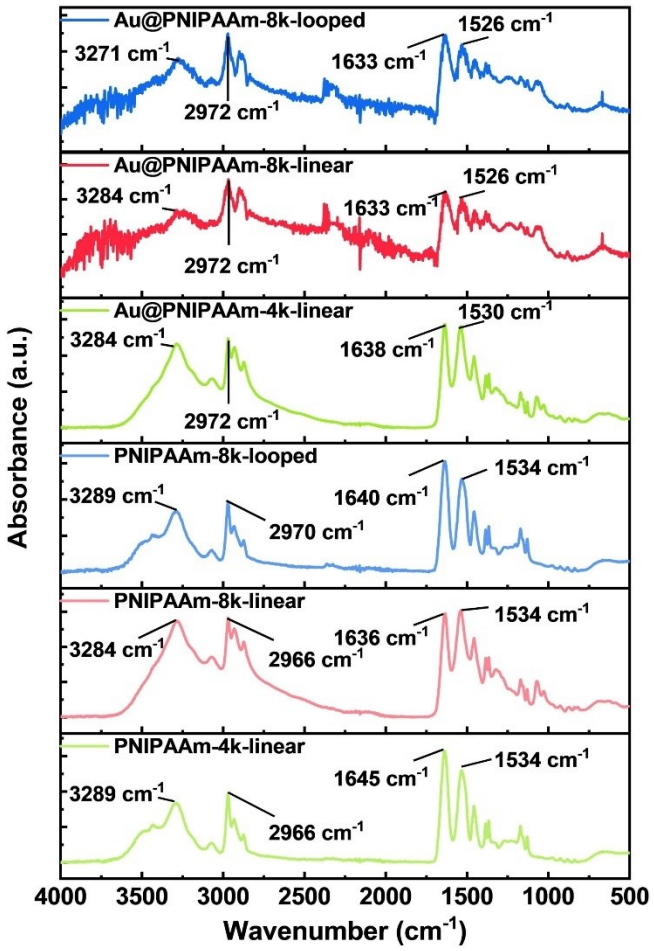

Fig. S4 FTIR spectra of PNIPAAm-4k-linear, PNIPAAm-8k-linear, PNIPAAm-8k-looped,

Au@PNIPAAm-4k-linear, Au@PNIPAAm-8k-linear, and Au@PNIPAAm-8k-looped.

GPC of Polymer

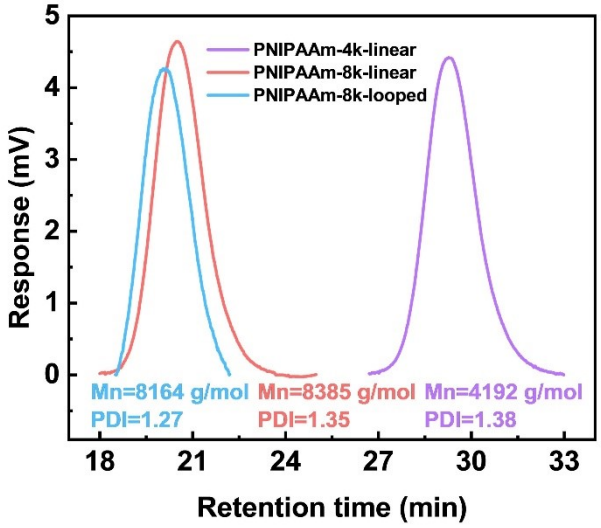

Fig. S5 GPC curves of PNIPAAm-4k-linear, PNIPAAm-8k-linear and PNIPAAm-8k-looped.

Size Distribution and Note on Polymer Bridging

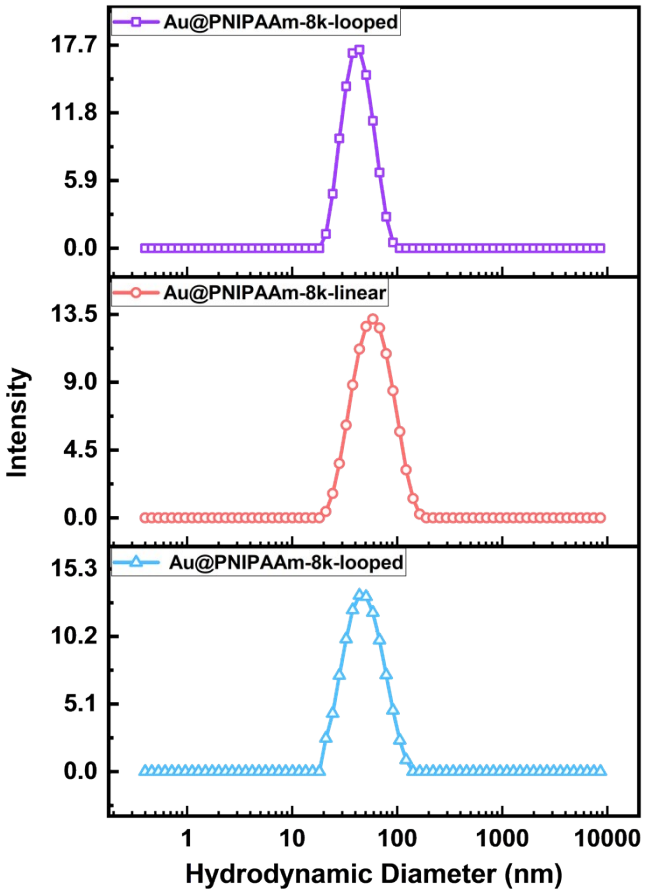

Fig. S6 The hydrodynamic diameter and nanoparticle distribution of Au@PNIPAAm-4k-linear,

Au@PNIPAAm-8k-linear, and Au@PNIPAAm-8k-looped measured in water.

DLS would be more sensitive to large aggregates. In particular, for Au@PNIPAAm-8k-looped, the grafting process might form polymer bridging, and once bridging occurred, the nanoparticles were connected by bridges, leading to some degree of aggregation or even precipitation[1]. The bridge formation rate was connected with the escape of one end sticker from the narrow-but-deep association well near the colloidal surface and the longer-range motion of the chain end to the other surface inhibited by stretching free energy [2]. On the one hand, the grafting strategy we employ was carried out in an extremely dilute nanoparticle solution, which could effectively reduce the long-range motion of the chain end to the other nanoparticle surface. On the other hand, the size distribution indicated the absence of any aggregates, which confirmed that the grafted PNIPAAm coated nanoparticles were well dispersed in water (Fig. S6).

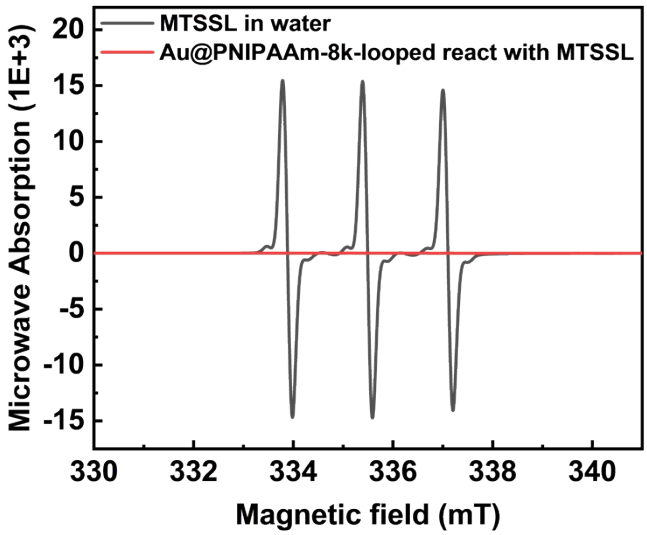

Fig. S7 Electron paramagnetic resonance spectra of Au@PNIPAAm-8k-looped reacted with MTSSL after purified.

Further, the probe molecule MTSL with paramagnetic signaling could react specifically and efficiently with thiol groups [3, 4]. After the reaction of Au@PNIPAAm-8k-looped with MTSL, the mixtures were purified. Fig. S7 showed that the mixture had no significant EPR signal, indicating that there was almost no free thiol groups present in the solution system of nanoparticles.

Calculations of theoretical contour length

The theoretical contour length of polymer often used to describe the length of a linear polymer chain in the ideal case, when the polymer chain is fully unfolded without any twisting or curling. This can be calculated using the following formula [5]:

$$L_{contour} = N \cdot l_0$$

where N is number of units in the polymer chain and l_0 length of each unit as expressed in the following equation:

$$N = \frac{M_n - M_x}{M_0}$$

$$l_0 = 2l\sin\frac{\theta}{2}$$

where M_n is polymer molecular weight, M_x is molar mass of the terminal functional groups, M_0 is molecular weight of structural units, l is bond length (0.154 nm for C-C bond), θ is bond angle (109°28′ for sp^3 hybridization).

Flow chart of dye loading and release

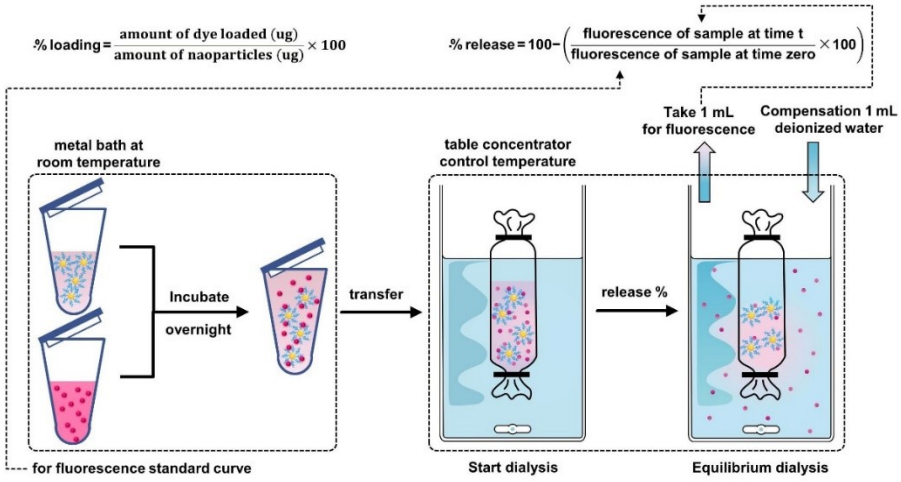

Fig. S8 Scheme of small molecule dye loading and release.

In the sample processing stage: the sample is first mixed with the fluorescent dye and subsequently incubated overnight at room temperature to ensure that the dye is fully bound to the sample.

Fluorescence measurement session: the mixture was encapsulated into a dialysis and the dialysis was placed in a beaker, the solution was submerged with 5 ml of water and stirred, and at a specific time point (t), 1 ml of the liquid was removed for the fluorescence intensity test and an equal volume of water was added to the system. The release of dye from the sample can be quantified by calculating the percentage release of fluorescence intensity.

Characteristics of Nanoparticles

Table S1. Characteristics of hydrodynamic diameter, polydisperse index in in DLS for bare and PNIPAAm-grafted AuNPs (errors: mean ± standard deviation, n=3 experimental replicated, NA represented not applicable).

Sample	$D_H^{25°C}$ (nm) [a]	$PDI^{25°C}$ (nm) [b]	$D_H^{45°C}$ (nm) [a]	$PDI^{45°C}$ (nm) [b]	$\frac{1}{2}d_s$ (nm) [c]
AuNPs	23.85	0.08	24.24	0.18	NA
Au@PNIPAAm-4k-linear	43.22	0.19	42.38	0.26	9.6
Au@PNIPAAm-8k-linear	63.64	0.34	50.55	1.02	19.4
Au@PNIPAAm-8k-looped	43.62	0.22	32.07	0.20	8.8

[a] Measured by DLS in distilled deionized water with superscripts indicating different temperatures equilibrated 15 min before measurement.
[b] Estimated from multiple DLS measurements for D_H at certain temperature.
[c] Calculated by D_H at 25 °C.

Table S2. Characteristics of localized surface plasmon resonance, zeta potential and chain density for bare and PNIPAAm-grafted AuNPs (errors: mean ± standard deviation, n=3 experimental replicated, NA represented not applicable).

Sample	*LSPR peak* (nm) [a]	$\zeta^{25°C}$ (mV) [b]	$\zeta^{45°C}$ (mV) [b]	σ (nm^{-2}) [b]
AuNPs	520.0	-43.21 ± 0.27	-38.52 ± 0.27	NA
Au@PNIPAAm-4K-linear	522.2	-23.06 ± 0.20	-19.51 ± 0.19	0.78
Au@PNIPAAm-8K-linear	522.8	-29.42 ± 0.56	-26.34 ± 1.21	0.64
Au@PNIPAAm-8K-looped	523.1	-32.40 ± 0.35	-28.43 ± 0.19	0.35

[a] Measured by UV-vis.
[b] Measured by DLS in distilled deionized water with superscripts indicating different temperatures equilibrated 15 min before measurement.
[c] Estimated from by HPLC.

Calculations of Relaxation Time

In a dynamic light-scattering experiment, we measure the $G_2(\tau)$, an optical intensity $I(t)$ correlation function rises and falls with time that describes the motion of colloidal particles [6]:

$$G_2(\tau) = \langle I(t)I(t+\tau)\rangle$$

which can be expressed as the integral of the product of the intensity at time (t) and the delay time ($t + \tau$) and τ is the lag time between the two time points.

Furthermore, the motions of the particles with respect to each other can be related by the electric field correlation function $G_1(\tau)$, which accounts for the associated particle motions and can be defined as:

$$G_1(\tau) = \langle E(t)E(t+\tau)\rangle$$

where, $E(\tau)$ and $E(t+\tau)$ represent the scattered electric fields at time (t) and ($t + \tau$)

The $G_1(\tau)$ and $G_2(\tau)$ can be normalized as $g_1(\tau)$ and $g_2(\tau)$, which can be coupled to each other by the Siegert relation [7]:

$$g_2(\tau) = B + \beta|g_1(\tau)|^2$$

where *B* is the baseline (~1) and *β* is the coherence factor that depends on detector area, optical alignment, and scattering properties of colloidal.

For polydisperse system, $g_1(\tau)$ can be represented as intensity-weighed integral over a distribution of decay rates $G(\Gamma)$ represented as:

$$g_1(\tau) = \int_0^\infty G(\Gamma) e^{-\Gamma_\tau d\Gamma}$$

The decay constant *Γ* (the inverse of the correlation time) is directly related to the diffusion behavior of colloidal (D_τ) as expressed in the following equation [8]:

$$D_\tau = \frac{\Gamma}{q^2}$$

$$\Gamma = \tau_c^{-1}$$

Where τ_c is the relaxation time and the Bragg wave vector *q* is proportional to solvent refractive index *n* as:

$$q = \frac{4\pi n}{\lambda} \sin\frac{\theta}{2}$$

Where *λ* is the wavelength of incident light and, *θ* is angle at which the detector is placed.

Therefore, $g_2(\tau)$ can be rewritten as:

$$g_2(\tau) = 1 + \beta e^{-2D_\tau q^2 \tau}$$

Which connects the particle motion with the measured fluctuations [9].

In additionally, the hydrodynamic radius (R_H), which can be defined as the radius of a hypothetical sphere that diffuses at the same rate as particle under investigation, can be obtained using the Stokes–Einstein equation [10]:

$$R_H = \frac{k_B T}{6\pi\eta D}$$

Where Boltzmann's constant k_B is 1.380 × 10^{-23} kg·m^2·s^{-2}·K^{-1}, *T* is the absolute temperature, and *η* is the solvent viscosity. The viscosity of water at 25 °C and 45 °C is 0.8903 mPa·s and 0.5972 mPa·s

respectively[11, 12]. λ is the wavelength (632.8 nm) and θ being the scattering angle (90°). The refractive index of water at 25 °C and 45 °C is 1.3325 and 1.3299 respectively[13, 14].

Table S3. Translational diffusion coefficients (D) and relaxation times (τ) of several groups of samples at 25°C and 45°C, corresponding temperature marked at superscript.

Sample	$D^{25\,°C}$ ($m^2 \cdot s^{-1}$)	$\tau^{25\,°C}$ (ms)	$D^{45\,°C}$ ($m^2 \cdot s^{-1}$)	$\tau^{45\,°C}$ (ms)
AuNPs	2.023E-11	14.12	3.252E-11	8.82
Au@PNIPAAm-4k-linear	1.135E-11	25.16	1.853E-11	15.48
Au@PNIPAAm-8k-linear	7.821E-12	36.52	1.622E-11	17.68
Au@PNIPAAm-8k-looped	1.182E-11	24.17	2.408E-11	11.91

The Variety of LSPR Peak and Absorption Intensity Mixing with Salt on Colloids

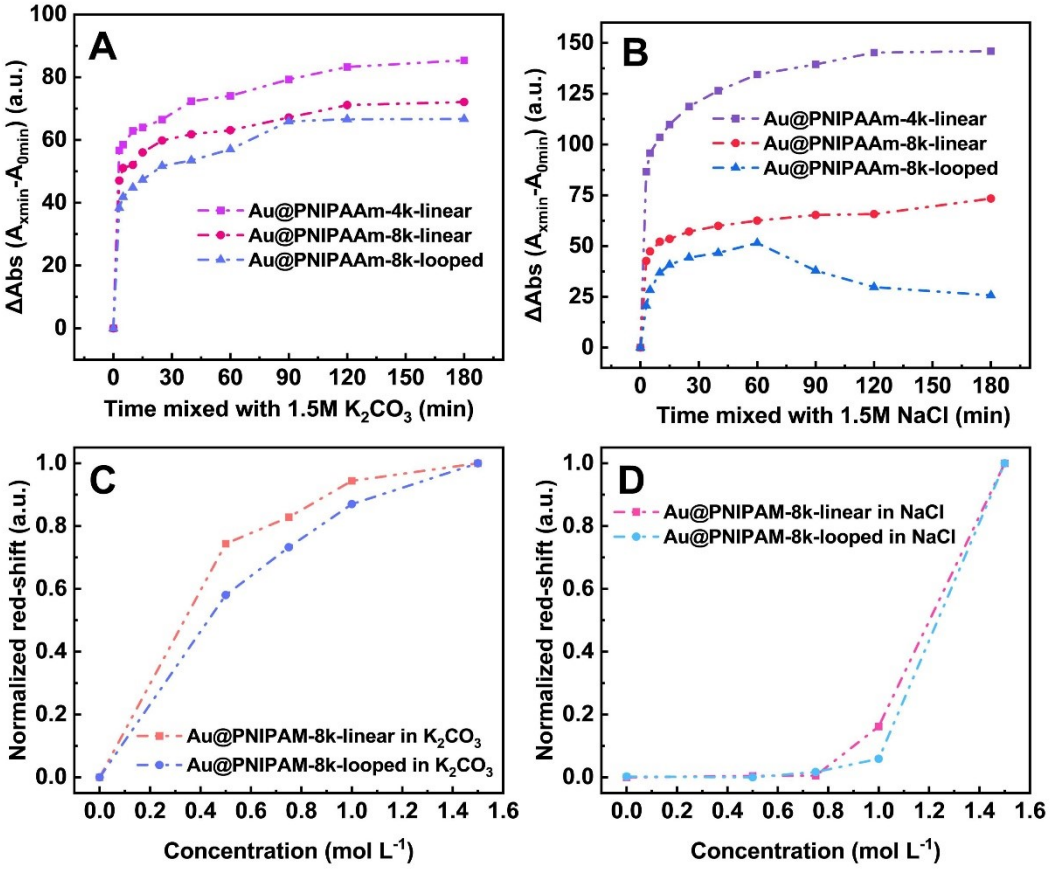

Fig. S9. The difference between the wavelength corresponding to the LSPR peak at moment x min and moment 0 min versus the time of mixing Au@PNIPAAm and K_2CO_3 (A) or NaCl (B). The normalized red-shift difference concentration of K_2CO_3 (C) or NaCl (D) mixing with Au@PNIPAAm.

Table S4. 5The LSPR peak positions ($Peak_{SPR}^{c_{salt}}$) of Au@PNIPAAm-8k-linear and Au@PNIPAAm-8k-looped in different salt concentrations.

Sample	c_{NaCl}^{*} (M)	$Peak_{SPR}^{c_{NaCl}}$ (nm)				
		$c_{NaCl}=0M$	$c_{NaCl}=0.5M$	$c_{NaCl}=0.75M$	$c_{NaCl}=1.0M$	$c_{NaCl}=1.5M$
Au@PNIPAAm-8k-linear	≤0.75	522.79	522.95	522.98	528.68	559.12
Au@PNIPAAm-8k-looped	≤1.0	523.10	522.98	523.54	524.93	556.01
Sample	$c_{K_2CO_3}^{*}$(M)	$Peak_{SPR}^{c_{K_2CO_3}}$ (nm)				
		$c_{K_2CO_3}=0M$	$c_{K_2CO_3}=0.5M$	$c_{K_2CO_3}=0.75M$	$c_{K_2CO_3}=1.0M$	$c_{K_2CO_3}=1.5M$
Au@PNIPAAm-8k-linear	<0.5	522.79	554.35	557.93	562.85	565.23
Au@PNIPAAm-8k-looped	<0.5	523.07	549.99	557.05	563.41	569.45

The Hysteresis Phenomenon of D_H

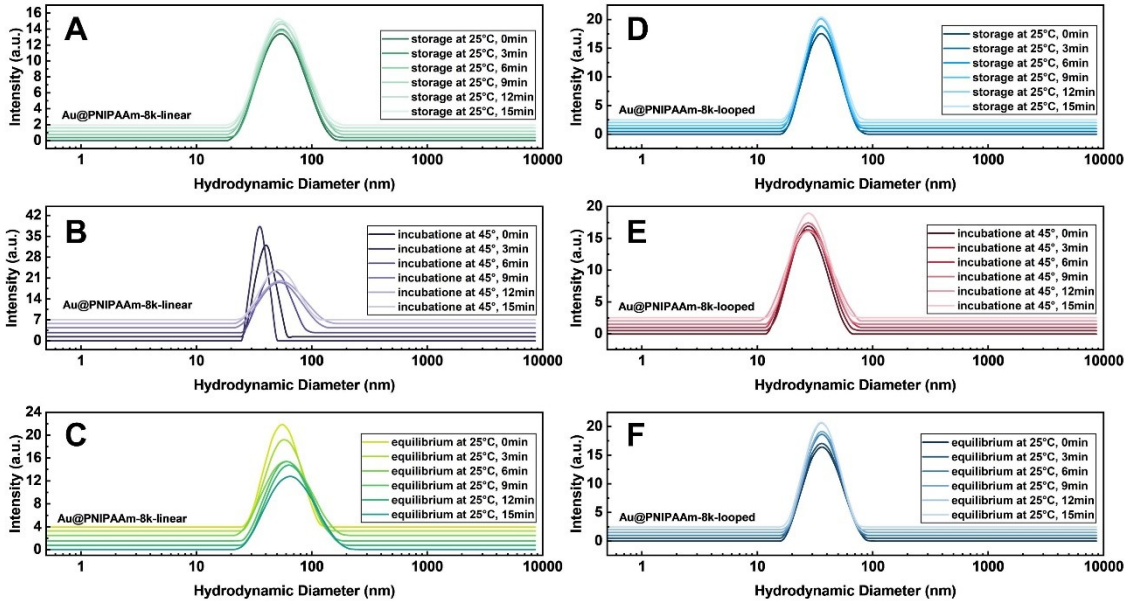

Fig. S10 The D_H of Au@PNIPAAm-8k-linear and Au@PNIPAAm-8k-looped first storage at 25 °C then heating to 45 °C incubation a period time and then cooling to 25 °C for equilibrium in a while (around 0.2 – 0.3 °C per minutes) recorded at the time.

REFERENCES

(1) Nayak, S.; Horst, N.; Zhang, H.; Wang, W.; Mallapragada, S.; Travesset, A.; Vaknin, D. Ordered Networks of Gold Nanoparticles Crosslinked by Dithiol-Oligomers. *Particle & Particle Systems Characterization* **2018**, *35* (8), 1800097

(2) Rezvantalab, H.; Larson, R. G. Bridging Dynamics of Telechelic Polymers between Solid Surfaces. *Macromolecules* **2018**, *51* (5), 2125-2137

(3) Li, Q.; Armstrong, Z.; MacRae, A.; Ugrinov, A.; Feng, L.; Chen, B.; Huang, Y.; Li, H.; Pan, Y.; Yang, Z. Metal–Organic Materials (MOMs) Enhance Proteolytic Selectivity, Efficiency, and Reusability of Trypsin: A Time-Resolved Study on Proteolysis. *ACS Appl. Mater. Interfaces* **2023**, *15* (7), 8927-8936

(4) Li, H.; Pan, Y.; Farmakes, J.; Xiao, F.; Liu, G.; Chen, B.; Zhu, X.; Rao, J.; Yang, Z. A sulfonated mesoporous silica nanoparticle for enzyme protection against denaturants and controlled release under reducing conditions. *J. Colloid Interface Sci.* **2019**, *556*, 292-300

(5) Gennes, P. G. d. Scaling Concepts in Polymer Physics. 1979.

(6) Berne, B. J.; Pecora, R. *Dynamic light scattering: with applications to chemistry, biology, and physics*; Courier Corporation, 2000.

(7) Siegert, A. J. F. *On the fluctuations in signals returned by many independently moving scatterers*; Radiation Laboratory, Massachusetts Institute of Technology, 1943.

(8) Arzenšek, D. Dynamic light scattering and application to proteins in solutions. *Seminar University of Ljubljana* **2010**, 1-18

(9) Burchard, W. Static and dynamic light scattering from branched polymers and biopolymers. In *Light Scattering from Polymers*, Berlin, Heidelberg, 1983//, 1983; Springer Berlin Heidelberg: pp 1-124.

(10) Pusey, P. *Correlation and light beating spectroscopy*; Plenum Press, New York, 1972.

(11) Korson, L.; Drost-Hansen, W.; Millero, F. J. Viscosity of water at various temperatures. *The Journal of Physical Chemistry* **1969**, *73* (1), 34-39

(12) Kestin, J.; Khalifa, H. E.; Sookiazian, H.; Wakeham, W. A. Experimental Investigation of the Effect of Pressure on the Viscosity of Water in the Temperature Range 10–150°C. *Berichte der Bunsengesellschaft für physikalische Chemie* **1978**, *82* (2), 180-188

(13) Robinson, G. W.; Cho, C. H.; Gellene, G. I. Refractive Index Mysteries of Water. *J. Phys. Chem. B* **2000**, *104* (30), 7179-7182

(14) Eisenberg, H. Equation for the Refractive Index of Water. *The Journal of Chemical Physics* **1965**, *43* (11), 3887-3892